Structural Asymmetry and Half-Site Reactivity in the T to R Allosteric Transition of the Insulin Hexamer†

Peter S. Brzović,‡,§ Wonjae E. Choi,‡ Dan Borchardt,‖ Niels C. Kaarsholm,⊥ and Michael F. Dunn*,‡

Departments of Biochemistry and Chemistry, University of California, Riverside, Riverside, California 92521-0129, and Novo Research Institute, Novo Alle, DK-2880 Bagsvaerd, Denmark

Received May 25, 1994; Revised Manuscript Received August 8, 1994®

ABSTRACT: The zinc–insulin hexamer, the storage form of insulin in the pancreas, is an allosteric protein capable of undergoing transitions between three distinct conformational states, designated T_6, T_3R_3, and R_6, on the basis of their ligand binding properties, allosteric behavior, and pseudo point symmetries [Kaarsholm, N. C., Ko, H.-C., & Dunn, M. F. (1989) *Biochemistry 28*, 4427–4435]. The transition from the T-state to the R-state involves a coil-to-helix transition in residues 1–8 of the B-chain wherein the ring of PheB1 is displaced by ~30 Å. This motion also is accompanied by small changes in the positions of A-chain residues and other B-chain residues. In this paper, one- and two-dimensional (COSY and NOESY) ^{1}H NMR are used to characterize the ligand-induced T to R transitions of wild-type and EB13Q mutant human zinc–insulin hexamers and to make sequence-specific assignments of all resonances in the aromatic region of the R_6 complex with resorcinol. The changes in the ^{1}H NMR spectrum (at 500 and 600 MHz) that occur during the T to R transition provide specific signatures of the conformation change. Analysis of the dependence of these spectral changes for the phenol-induced transition as a function of the concentration of phenol establish (1) that the interconversion of T_6 and R_6 occurs via a third species assigned as T_3R_3 and (2) that the system shows both negative and positive cooperative allosteric behavior. One- and two-dimensional COSY and NOESY studies show that, in the absence of phenolic compounds, anions act as heterotropic effectors that shift the distribution of hexamer conformations in favor of the R-state with the order of effectiveness, $SCN^- > N_3^- \gg I^- \gg Cl^-$. Analysis of one- and two-dimensional spectra indicate that with wild-type insulin, SCN^- and N_3^- give T_3R_3 species, whereas the EB13Q mutant gives an R_6 species. An allosteric model for the insulin T to R transition based on the structural asymmetry model [Seydoux, F., Malhotra, O. P., & Bernhard, S. A. (1974) *CRC Crit. Rev. Biochem. 2*, 227–257] is proposed that explains the negative and positive allosteric properties of the system, including the role of T_3R_3 and the action of homotropic and heterotropic effectors.

The concerted (MWC) model[1] for allosteric interactions proposed by Monod et al. (1965) is a symmetry-driven model wherein positive cooperative ligand binding to an oligomeric protein arises as a consequence of a symmetry-conserved interconversion between two alternative quaternary conformations (Matthews & Bernhard, 1973). If the two conformations display different ligand binding affinities, then under certain circumstances, the binding of ligands will show a positive cooperativity that can be modulated by negative and positive effectors. Because the MWC model is constrained to two different quaternary conformations with protomers of identical conformation making up each state, it follows that symmetry within the oligomeric protein must be conserved, and therefore, both ligand binding sites and intersubunit interactions within the complex must be identical (Matthews & Bernhard, 1973; Seydoux et al., 1974).

One shortcoming of the MWC model is the failure to explain negative homotropic interactions (Conway & Koshland, 1968; Corwin & Fanning, 1968). Negative cooperative interactions require the presence of ligand binding sites of differing affinities within a single oligomeric state and, therefore, a loss of symmetry in the protein complex. Most current alternatives to the MWC model are explicitly designed to allow quaternary conformations for partially liganded states which are of low symmetry or are asymmetrical (Koshland et al., 1966; Koshland, 1970). The sequential model proposed by Koshland et al. (1966), the KNF model, can explain both positive and negative homotropic interactions, but the symmetry properties of the oligomeric protein are not an essential component of the model. Alternatively, Matthews and Bernhard (1973) and Seydoux et al. (1974) have taken into consideration the observed symmetry of allosteric oligomeric proteins in designing a model that can accommodate both positive and negative cooperative behavior. In reviewing the literature on the symmetry properties of oligomeric proteins, Matthews and

† Supported by NIH Grants R01-DK42124 and 2T-DK07310 and a gift from the Novo Research Institute.

* To whom correspondence should be addressed.

‡ Department of Biochemistry, University of California, Riverside.

§ Present address: Department of Biochemistry, Health Science Building, University of Washington, Seattle, WA 98195.

‖ Department of Chemistry, University of California, Riverside.

⊥ Novo Research Institute.

® Abstract published in *Advance ACS Abstracts,* October 1, 1994.

[1] Abbreviations: T and R are used throughout to designate insulin forms, respectively, with extended (T) and α-helical (R) conformations for residues 1–8 of the B chain. T_6, T_3R_3, and R_6 are used throughout to designate the three general forms of the insulin hexamer. T_3T_3' and R_3R_3' are used to designate the conformations of hexamers with one 3-fold axis and three pseudo 2-fold axes of symmetry, while $T_3{}^oR_3{}^o$ is used to designate hexameric species with only a single, 3-fold axis of symmetry (Kaarsholm et al., 1989). The site-specific mutation of residue GluB13 to Gln in human insulin is designated as EB13Q. COSY, two-dimensional correlation spectroscopy; NOESY, two-dimensional nuclear Overhauser and exchange spectroscopy; DQF, double-quantum filtered; TPPI, time–proportional phase incrementation; ppm, parts per million; CD, circular dichroism; MWC, concerted model of allostery (Monod et al., 1965); KNF, sequential model of allostery (Koshland et al., 1966); SMB, structural asymmetry model for negative and positive cooperativity (Seydoux et al., 1974).

0006-2960/94/0433-13057$04.50/0

Bernhard (1973) noted the high preponderance of deviations from exact 2-fold symmetry within oligomeric proteins made up of subunits with identical covalent sequences. The propensity to assemble even-numbered oligomers from asymmetric dimers implies that pseudoisologous interactions are important in protomer–protomer assembly, and as a consequence, even-numbered oligomers are almost always characterized by what Seydoux et al. (1974) define as "suboptimal intramolecular symmetry" where there is a "... pairwise asymmetry in subunit conformation". With this asymmetry in mind, they proposed a cooperativity model (the SMB model) based on the assumptions that (1) suboptimal symmetry in the oligomer can give rise to site heterogeneity and (2) there can be conformational isomerization between quaternary states of optimal and suboptimal symmetry. Depending on model parameters, the SMB model is capable of explaining both positive and negative cooperativity. Positive cooperative behavior in this model arises from ligand binding interactions that drive the conformational transition in favor of the conformation state(s) of higher ligand affinity in a manner similar to that of the MWC model. Because structural constraints in the oligomer cause different classes of sites to exist simultaneously, the postulation of homotropic negative cooperative interactions is not a feature of the model. Negative cooperative behavior in this model is a direct consequence of *structural asymmetry* arising from the suboptimal symmetry of the protein. In the extreme, this model predicts that half-site reativity will be manifest as a consequence of the assembly of the oligomer from asymmetric dimeric units.

The insulin hexamer provides a unique system with which to investigate these ideas. The hexamer is assembled from three dimers related by an exact 3-fold axis of symmetry (Figure 1). Two Zn^{2+} ions are located on the 3-fold axis, and each is coordinated by three symmetry-related B10 histidine residues from separate monomeric units. However, monomeric units of each dimer exhibit deviations from exact 2-fold symmetry, and under certain conditions, pseudo 2-fold symmetry may be completely lost. X-ray crystallographic studies have characterized three different states of the protein complex that are characterized by remarkable conformational differences (Figure 1; Blundell et al., 1972; Baker et al., 1988; Smith et al., 1984; Derewenda et al., 1989, 1991; Smith & Dodson, 1992a,b; Bentley et al., 1992; Ciszak & Smith, 1994). These quaternary conformations have been designated T_3T_3', T_3R_3, and R_3R_3' on the basis of their ligand binding properties, allosteric properties, and pseudo point symmetries (Kaarsholm et al., 1989). For expediency, these structures have been abbreviated by most workers as T_6, T_3R_3, and R_6 in the recent literature. The T_6 and R_6 forms exhibit pseudo point symmetry; each has an exact 3-fold symmetry axis and three approximate dyad axes perpendicular to the 3-fold axis. Deviations from exact 2-fold symmetry are the consequence of small conformational differences within each dimeric unit of the hexamer. The T_3R_3 form of the hexamer contains only a single 3-fold symmetry axis but lacks the pseudo dyad axes, and therefore, T_3R_3 hexamers are composed of asymmetric dimeric units.

In the T-state, residues 1–8 of the insulin B-chain take up an extended conformation (Figure 1). The Zn^{2+} ions reside in a shallow depression at each end of the hexamer. Three water molecules complete the octahedral ligand field (Baker et al., 1988). The interconversion to the R-state causes residues 1–8 in the B-chain to adopt an α-helical conformation in which the phenyl ring of the PheB1 moves by nearly 30 Å (Derewenda et al., 1989). This conformational change creates a hydrophobic cavity (the phenolic pockets) located at the dimer interface of each monomer, which is large enough to accommodate a variety of small organic molecules including phenol, various substituted phenols, certain naphthalenes, and cyclooctanol (Brader et al., 1992; Choi et al., 1993). The new helical segments pack in around the HisB10 sites and constrain the ligand field surrounding the Zn^{2+} ion to either a tetrahedral or a five-coordinate geometry (Derewenda et al., 1989; Brader et al., 1990, 1991; Brader & Dunn, 1991). The fourth position may be occupied by a large number of different anions. Thus, the T_6 to R_6 conformational transition is driven by the binding of ligands both to the phenolic pockets and to the Zn^{2+}–metal ions (Brader et al., 1992; Choi et al., 1993). Smaller conformational changes occur throughout both the remainder of the B-chain and the A-chain. Although these regions of the structure exhibit similar backbone conformations in both the T- and R-states, there are small conformational changes throughout.

The T_3R_3 hexamer is composed of asymmetric dimers wherein each dimer contains one insulin molecule in a T-like conformation with the other in an R-like conformation (Smith et al., 1984; Ciszak & Smith, 1994). Thus, the 3-fold symmetry-related dimers give a hexameric species in which one end of the hexamer has the T conformation (a T_3 unit) while the other end has the R conformation (an R_3 unit). The interactions that stabilize the T_3R_3 conformation in the crystalline state are not entirely clear (Chothia et al., 1983; Ciszak & Smith, 1994). Evidence consistent with the existence of the T_3R_3 conformation in solution has been derived primarily from CD studies (Wollmer et al., 1987, 1989), rapid kinetic measurements (Kaarsholm et al., 1989), and UV–visible absorbance spectroscopy (Brader et al., 1991; Choi et al., 1993). However, all of this evidence has been ambiguous. Herein, we report ^1H NMR studies that characterize a variety of T_3R_3 ligand complexes in solution. These studies establish that the stabilization of a T_3R_3 structure arises from structural asymmetry that is mediated by ligand binding. Furthermore, we propose that the suboptimal symmetry of the insulin hexamer can give both positive and negative allosteric behavior in ligand binding and that the SMB model for allostery provides a satisfying explanation for the allosteric properties of the insulin hexamer.

EXPERIMENTAL METHODS

Materials. Metal-free recombinant human insulin and the recombinant human insulin mutant EB13Q were gifts supplied by the Novo Research Institute (Bagsvaerd, Denmark). $ZnSO_4$ (Mallinckrodt), $CaSO_4$ (Mallinckrodt), NaCl (Fisher Scientific), NaI (Matheson, Coleman, and Bell), NaN_3 (Sigma), 2,2′:6′–2″-terpyridine (Terpy) (Sigma), KSCN (Mallinckrodt), resorcinol (Aldrich), and *m*-cresol (Aldrich) were used without further purification. $^2H_2SO_4$, 40% NaO^2H, phenol-d_6, 2,2-dimethyl-2-silapentane-5-sulfonate-*2,2,3,3-d*$_4$ (DSS), and ^2H_2O (99.8% ^2H) were purchased from Aldrich and used without further purification.

Sample Preparation for ^1H NMR. The concentration of stock solutions prepared in D_2O were determined spectrophotometrically with an HP 8452 UV–visible spectrophotometer using the appropriate extinction coefficients for each molecule; *m*-cresol ($\epsilon_{275} = 2.00 \times 10^3$ M^{-1} cm^{-1}), resorcinol ($\epsilon_{276} = 2.00 \times 10^3$ M^{-1} cm^{-1}), phenol-d_6 ($\epsilon_{270} = 1.58 \times 10^3$ M^{-1} cm^{-1}), and insulin ($\epsilon_{280} = 5700$ M^{-1} cm^{-1}) (Porter, 1953). The concentration of zinc was determined spectrophotometrically as previously described (Palmeri et al., 1988) using the chromophoric chelator Terpy (bis Zn^{2+}–Terpy complex, ϵ_{333}

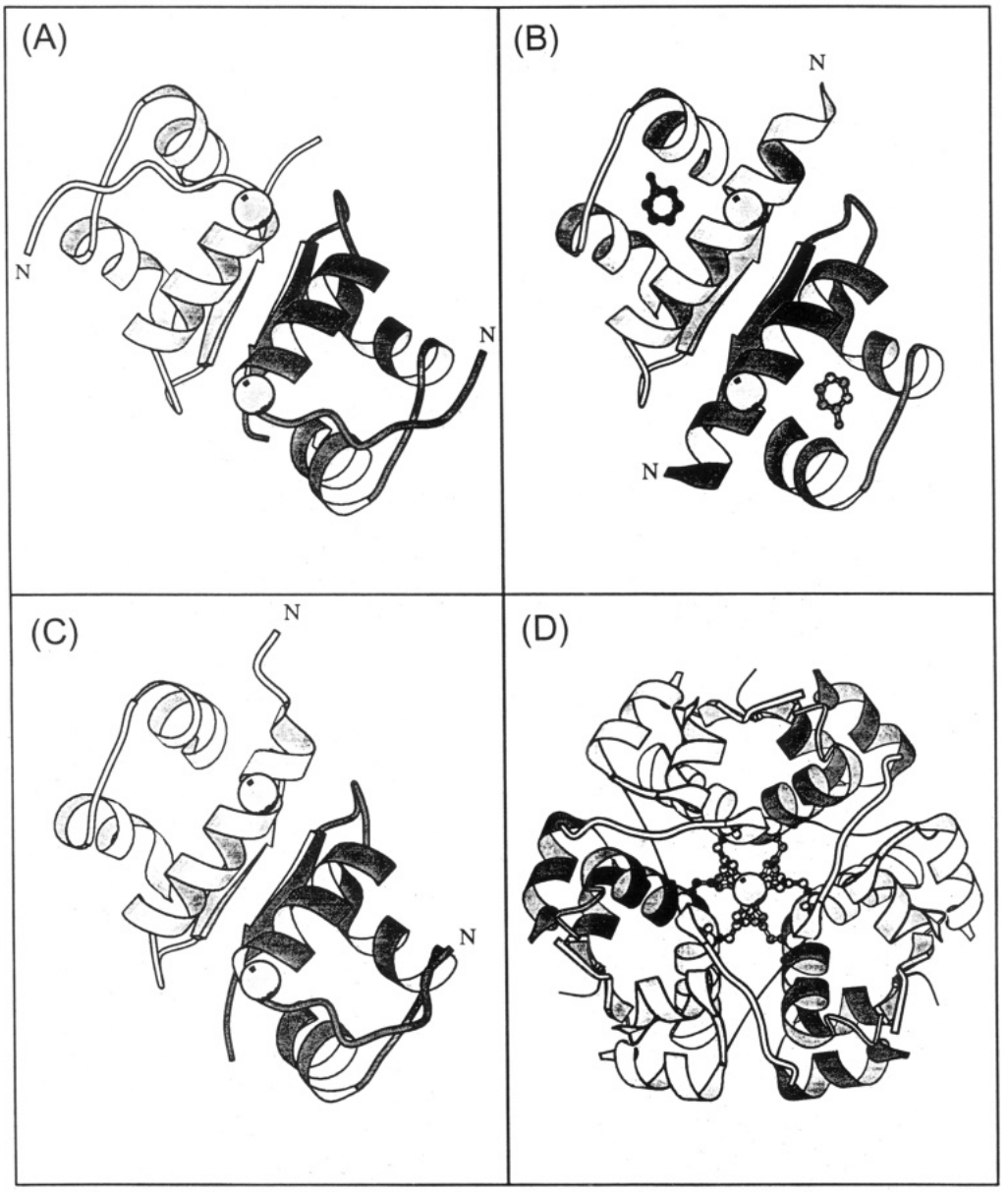

FIGURE 1: Illustrations depicting the symmetry properties and conformation transitions of the insulin hexamer. Insulin dimers, which comprise the asymetric unit in crystals of insulin hexamers, are shown for the T_6, T_3R_3, and R_6 conformational states of the insulin hexamer. The two Zn^{2+} ions in the foreground lie on the exact 3-fold axis which relates dimers within the hexamer. One of the three pseudo 2-fold symmetry axes present in the T_6 and R_6 states is oriented perpendicular to the plane of the paper. The N-terminal ends of the insulin B-chain have been labeled to highlight the nature and extent of the observed conformational changes in this region of the protein. (A) T-state dimer. (B) R-state dimer with phenol molecules positioned in the pockets. (C) Dimer with mixed T- and R-states that correspond to the T_3R_3 hexamer. Note the loss of the pseudo 2-fold symmetry axis. (D) View looking down the 3-fold symmetry axis of the T_6 insulin hexamer to illustrate the assembly of the insulin hexamer from dimeric units. The HisB10 ligands at each metal site are also shown. (Figures created with the program Molscript; Kraulis, 1991.)

$= 4.1 \times 10^4$ M^{-1} cm^{-1}). Zn^{2+} and Ca^{2+} ions were added at stoichiometric ratios of 2 Zn^{2+}:1 Ca^{2+}:6 insulin monomers. Ca^{2+} was added to help drive the assembly of the insulin hexamer by binding to the central GluB13 binding site (Palmeri et al., 1988) and to ensure segregation of Zn^{2+} to the HisB10 sites. The pH* of the solution (the direct meter reading) was adjusted with $^2H_2SO_4$ in order to avoid introducing unwanted anions which may coordinate to the Zn^{2+} ion in the insulin hexamer and complicate the interpretation of results.

^1H NMR Spectroscopy. Samples for NMR experiments were typically 2–5 mM insulin monomer. One-dimensional ^1H NMR spectra and two-dimensional magnitude mode NOESY and COSY spectra were collected on a GN-500 spectrometer equipped with a Nicolet 1280 computer. For both one- and two-dimensional spectra, the probe was thermostated at 25 °C. Chemical shifts are reported in parts per million relative to the water peak (4.77 ppm). The spectra consist of an average of 64 transients made up of 32K data points with a sweep width of ±3000 Hz. Presaturation was used between acquisitions to suppress the HOD signal. Two-dimensional spectra (256 or 512 t_1 increments by 2048 t_2 data points) were collected with a sweep width of either 5000 (magnitude mode) or 6579 Hz (phase-sensitive mode) and a recycle time of approximately 2 s between acquisitions. Sixty-four scans were averaged for each t_1 increment. Phase-sensitive NOESY (Bodenhausen et al., 1984) and double-quantum filtered COSY (Rance et al., 1983) experiments were collected in the time–proportional phase incrementation (TPPI) (Marion & Wüthrich, 1983) mode on a Bruker AMX 600 MHz spectrometer (Novo Nordisk). Two-dimensional data sets were zero-filled to 2K × 2K and processed with a standard sine-bell function in both dimensions for the

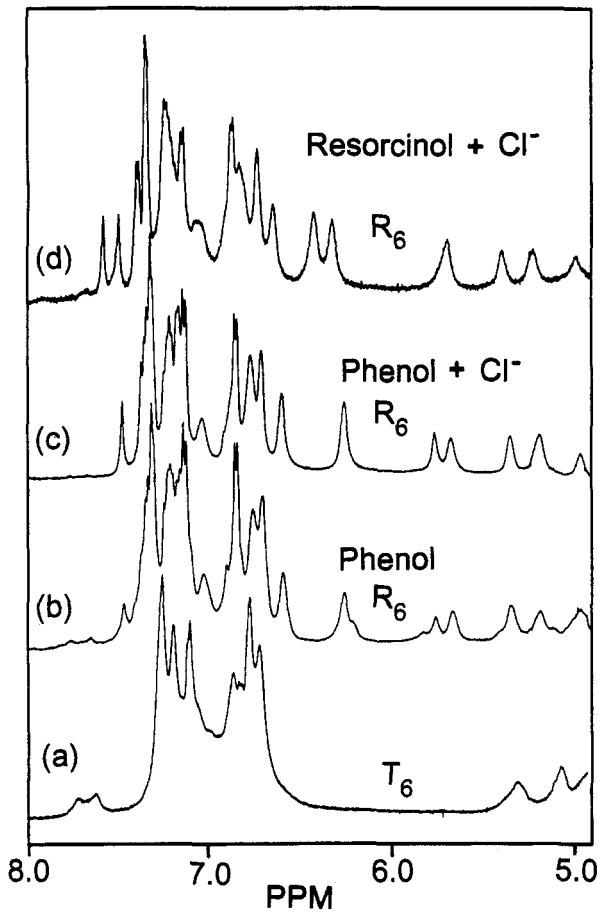

FIGURE 2: Effects of ligands on the 5.0–8.0 ppm region of the 500 MHz ^{1}H NMR spectrum in ^2H_2O of wild-type zinc–calcium–insulin hexamer at pH* 8.0 and 25 °C. All samples consist of a [Zn^{2+}]:[Ca^{2+}]:[insulin monomer] ratio = 2:1:6; [insulin monomer] = 3 mM. (a) Zn (II)–T_6. (b) Zn(II)–R_6 phenolate ion complex formed in the presence of 20 mM phenol-d_6 with no added inorganic monoanions. (c) Zn(II)–R_6 chloride ion complex formed in the presence of 20 mM phenol-d_6 and 50 mM NaCl. (d) Zn(II)–R_6 chloride complex formed in the presence of 3 mM resorcinol and 50 mM NaCl. The resonances at 6.45 and 7.1 ppm are due to the ring protons of resorcinol.

magnitude spectra or a squared sine-bell function phase-shifted by 65° in both dimensions for the phase-sensitive data. A mixing time of 150 ms was used for the NOESY experiments.

RESULTS

^{1}H NMR Spectra Changes Associated with Interconversion of Zn(II)–T_6 and Zn(II)–R_6. In ^2H_2O at pH* 8.0, the aromatic region of the ^{1}H NMR spectrum of the Zn(II)–T_6 hexamer with Ca^{2+} coordinated to the GluB13 site (Figure 2a) is characterized by at least two broadened envelopes of resonances centered at 5.10 and 5.35 ppm and an envelope of broadened resonances derived from three Phe, four Tyr, and two His residues located between 6.50 and 7.80 ppm. The HisB5 and HisB10 ring C2 protons are located at 7.74 and 7.63 ppm, respectively (Palmieri et al., 1988; Bradbury et al., 1980). The line widths of these resonances are broader than expected for a 36 000-Da protein (compare with Figure 2c), indicating that the T-state oligomer undergoes exchange broadening. Such line broadening may be caused (1) by exchange between multiple conformations of the T-state, (2) by exchange of dimeric subunits between hexamers, and (3) perhaps by the formation of higher order aggregates at the high insulin concentrations used in the NMR studies (Wüthrich, 1986).

^{1}H NMR spectra of the phenol-induced Zn(II)–R_6 hexamer with Ca^{2+} bound to the GluB13 site are presented in Figure 2, spectra b and c. The spectrum in Figure 2b was measured under conditions where phenol from solution is bound both to the phenolic pocket and to zinc as the fourth ligand at the HisB10 sites (Brader et al., 1991; Choi et al., 1993). In Figure 2c, the presence of the chloride ion in solution results in the displacement of phenolate from the metal site and the coordination of chloride ion to Zn(II) in the fourth tetrahedral position (Choi et al., 1993). It is clear for both R-state complexes that the protein conformational transition from the T- to R-state and the accompanying transformation of the HisB10 metal site geometry from octahedral to tetrahedral causes large perturbations in the chemical shifts and line widths of virtually every resonance between 5.0 and 8.0 ppm (Roy et al., 1989; Brader et al., 1991, 1992). Similar alterations occur in the aliphatic region of the spectrum (data not shown). Inspection of Figure 2b indicates the presence of two hexamer populations, one minor, when the phenolate ion is the anion coordinated to the HisB10 zinc sites. Several resonances appear to have shoulders (e.g., the peaks at 5.36 and 6.30 ppm) or are associated with minor resonances (resonances at 5.16 and 6.33 ppm) in addition to the persistence of the His C2 resonances at 7.63 and 7.74 ppm. Addition of chloride ion to the solution effectively eliminates these features. The presence of these features in the phenolate ion complex suggests that the hexamer exists in two, slowly interconverting forms and that replacement of phenolate by chloride ion drives the hexamer essentially to a single form. The conversion from Zn(II)–T_6 to the phenolate ion Zn(II)–R_6 complex causes many of the aromatic resonances to sharpen. Replacement of phenolate by chloride ion results in further sharpening of these resonances. These spectral changes are consistent with an R_6 structure that exists primarily in a single conformation and does not experience the same degree of exchange broadening observed for the T-state structure.

Sequence-Specific ^{1}H Assignments for the Aromatic Region of Zn(II)–R_6 Hexamer. Figure 3 compares the phase-sensitive COSY (A) and NOESY (B) spectra of the resorcinol-induced Zn(II)–R_6 chloride ion complex at pH* 8.0. A corresponding 1-D spectrum is shown in Figure 2d. Comparison of this spectrum with the spectrum of the Zn(II) R-state formed from a mutant insulin species in which TyrB16 has been replaced with histidine unambiguously identifies resonances at 6.33 and 6.85 ppm as belonging to TyrB16 (data not shown). This assignment provides a foothold for utilizing the pattern of COSY and NOESY cross peaks to assign the remainder of the aromatic region in a manner consistent with the observed aromatic spin systems (Wüthrich, 1986) and the X-ray structures of the R_6 complex (Derewenda et al., 1989; Smith & Dodson, 1992a,b). These assignments are summarized in Table 1. The insolubility of the insulin hexamer below pH 7.0 presently precludes a more direct approach to the determination of sequence-specific assignments.

Several features of the 2-D data are worth considering in greater detail. (1) There exists a strong NOE between TyrB16 and another aromatic residue located at 6.65 and 6.83 ppm. The crystal structure shows that TyrB26 is located within 4 Å of TyrB16 and the COSY cross peaks are consistent with this assignment (G. D. Smith, private communication). B26, in turn, exhibits strong NOE cross peaks to an aromatic residue at 6.91, 7.08, and 7.18 ppm. TyrB26 is located in a region of anti-parallel β-sheet that forms part of the monomer–monomer interface and is positioned within 4 Å of PheB24, both within a single monomer and across the monomer–

Table 1: Sequence-Specific Assignments of Proton Resonances for Spectrum of Zn(II)–R_6 Insulin Hexamer in Presence of 0.5 mM Ca^{2+}, 50 mM Chloride, and 6 mM Resorcinol[a]

aromatic protons			
residue	ppm	proton	assignment criteria
TyrB16	6.33	ring 3,5	comparison of human wild type with YB16H mutant
	6.85	ring 2,6	
TyrB26	6.65	ring 3,5	strong NOE to B16 ring
	6.83	ring 2,6	
TyrA19	6.74	ring 3,5	NOEs to aliphatic protons
	7.26	ring 2,6	
TyrA14	6.87	ring 3,5	line shape, few NOEs detected
	7.15	ring 2,6	
PheB24	6.91		COSY pattern and NOE cross peak to B26 (see text).
	7.08		
	7.18?		
PheB25	7.18		COSY pattern, NOEs to aliphatic protons, small chemical shift dispersion (see text)
	7.25		
	7.20?		
PheB1	7.40		sharp line widths, few NOEs to aliphatic region (see text)
	7.33		
	?		
HisB5	7.58	ring C2	strong NOEs to B16 and to resorcinol
	5.70	ring C4	weak NOE to C2 proton
HisB10	7.50	ring C2	chemical shift, NOE between C2 and C4 (see text)
	7.35	ring C4	

aliphatic protons between 5 and 6 ppm		
possible identity	ppm	assignment criteria
AsnB3 (Cα)?	5.40	one COSY cross peak to an aliphatic β-proton (see text)
PheB24 (Cα)	5.23	one COSY cross peak to an aliphatic β-proton, NOE cross peak to the ring of B24 (see text)
PheB25 (Cα)	5.00	one COSY cross peak to an aliphatic β-proton, NOE cross peak to the ring of B25 (see text)

[a] Parameters: SW, 6579 Hz, 10.96 ppm; SF, 600.14 MHz; H_2O offset, 4.77 ppm (center of spectrum).

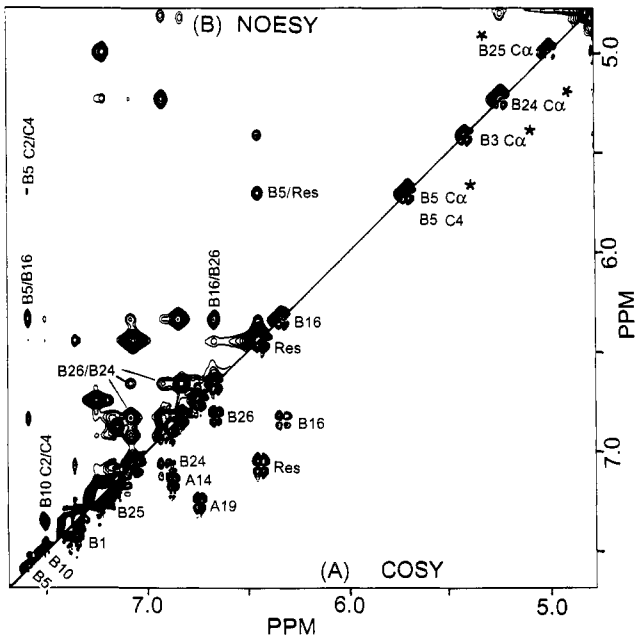

FIGURE 3: Comparison of the 600 MHz DQF phase-sensitive COSY (A) and NOESY (B) spectra of the 5.0–7.7 ppm region of the wild-type Zn(II)–R_6 chloride ion complex formed with resorcinol and Ca^{2+} in ^2H_2O at pH* 8.0 and 25 °C. COSY and NOESY cross peak and diagonal peak sequence-specific assignments are indicated. The logic for these assignments is given both in the text and in Table 1. Peaks due to resorcinol are designated Res. Assignments designated by an asterisk (*) are tentative (viz., the peaks at 5.0, 5.23, and 5.40 and the ring proton resonances for TyrA14, TyrA19, and PheB1, see text and Table 1). [Zn^{2+}]:[Ca^{2+}]:[insulin monomer] = 2:1:6; [insulin monomer] = 3 mM; [NaCl] = 50 mM.

monomer interface. (2) The COSY spectrum shows that the resonances of the two remaining Phe residues (PheB25 and PheB1) are centered at ~7.22 and ~7.35 ppm; these resonances show little chemical shift dispersion of the aromatic protons, and the chemical shifts are closer to the random coil chemical shifts expected for Phe residues (Wüthrich, 1986). PheB1 and, to a lesser extent, PheB25 are located on the surface of the insulin hexamer and would be expected to have some degree of rotational freedom. Although the crystal structures (Derewenda et al., 1989; Smith & Dodson, 1992a,b) of the R_6 hexamer show the side chain of B25 is oriented on the opposite side of the β-sheet from both B24 and B26, weak NOE cross peaks should be observed between these residues. The detection of such cross peaks is consistent with this reasoning and allows the assignment of resonances located at 7.18 and 7.25 ppm to PheB25. In contrast, no cross peaks are observed between the remaining Phe ring, PheB1, and other aromatic protons. PheB1 is located at the N-terminal of the R-state B-chain α-helix and is too distant from other aromatic residues to exhibit NOE cross peaks. (3) TyrA14 is positioned on the surface of the insulin hexamer away from other aromatic residues and is expected to exhibit considerable rotational freedom. The resonances observed at 6.87 and 7.15 ppm show very narrow line widths and a doublet splitting pattern in the 1-D spectra, a very strong cross peak in the COSY spectra, and very few NOEs with other side chain residues in the oligomeric protein, especially other aromatic residues. These features are consistent with the assignment of the 6.87 and 7.15 ppm resonances to TyrA14. Although TyrA19 is exposed to the solvent, the ring is oriented toward the interior of the monomeric subunit. As a result, the TyrA19 resonances are expected to be broader than the A14 signals and to exhibit a greater number of NOEs in the aliphatic region of the spectrum. This is precisely what is observed for the resonances located at 6.74 and 7.26 ppm. (4) The C2 and C4 ring protons of the two His residues are well-resolved and are assigned based on the observed pattern of NOE cross peaks (Table 1). TyrB16 shows a strong NOE cross peak to a His C2 proton

located at 7.58 ppm. The crystal structures show that formation of the R-state brings HisB5 within NOE contact of TyrB16. HisB5 also forms part of the binding pocket for the aromatic ligand. As a result, the C4 ring proton of HisB5 is greatly shifted upfield (see below) to 5.70 ppm. This large perturbation in chemical shift is due to an anisotropic ring current effect between HisB5 and the binding of the aromatic ligand (resorcinol). The absolute extent of the shift is ligand-dependent, indicating that the disposition of side chains in the ligand binding pocket is flexible and the pocket adapts to accommodate structural differences that exist between the various aromatic ligands. (5) In the R-state, the HisB10 ring protons are located at 7.35 and 7.50 ppm. The arrangement of B10 rings in the Zn(II) site brings the C2 and C4 ring protons from B10 residues in different monomers in NOE contact with one another. (6) The resonances that arise from resorcinol are located at 6.44 and 7.08 ppm. As expected from the crystal structure, NOE cross peaks are observed between resorcinol and HisB5.[2]

Based on chemical shifts, peak areas, the absence of COSY cross peaks with the aromatic protons, and the presence of COSY cross peaks with the aliphatic region, the resonances observed between 5 and 6 ppm have been provisionally assigned to Cα backbone protons. The strong cross peaks observed at 6.90 and 7.23 ppm and the observed pattern of NOE cross peaks with other aromatic residues are consistent with the assignment of the resonances at 5.00 and 5.23 ppm to the Cα protons of PheB24 and PheB25, respectively, located in the antiparallel β-sheet that forms part of the monomer–monomer interface. The remaining resonances at 5.40 and ~5.70 ppm exhibit strong NOE cross peaks in the aromatic region only to resorcinol. The resonance at ~5.70 ppm is actually the superposition of two resonances, one of which has been assigned to the C4 ring proton of HisB5. These resonances are clearly resolved when either phenol or *m*-cresol is bound to the hexamer in place of resorcinol (see below). If cyclohexanol is used to induce the T to R conformational change, then the resonance assigned to the C4 proton of B5 is conspicuously absent from this region of the spectrum (data not shown). The remaining resonances are still observed in the presence of cyclohexanol, indicating that anisotropic ring current effects from the aromatic ligand are not responsible for the large downfield shifts of these peaks. However, weak NOE cross peaks or cross peaks that arise from spin diffusion are observed between the peak at 5.4 ppm and PheB1 and between the two Cα peaks. This observation is consistent with the assignment of these two resonances to residues located in the extended helix comprised of residues B1–B8, the region of the protein undergoing the largest conformational change. One explanation consistent with these observations is that the ring of B5 induces spectral shifts in nearby Cα protons. The X-ray structure indicates that the edge of the HisB5 ring, in particular the δN, is within 4 Å of its own Cα proton. Although other possibilities cannot be eliminated, the weak NOEs observed between the peak at 5.4 ppm and the PheB1 peak at ~7.35 ppm indicate that the peaks may arise from the Cα protons of either AsnB3 or GlnB4.

[2] However, cross peaks to HisB10 are also evident. There are two possible explanations for this observation: (a) the position of resorcinol in the ligand binding pocket brings it within NOE contact with HisB10 or (b) the excess resorcinol present in solution permits displacement of chloride ion and direct ligation of resorcinol to the metal site. Resorcinol is a much better ligand for the Zn–metal site than phenol. Similar behavior has been observed for the binding of resorcinol to the metal in the Co(II) R-state hexamer, albeit at higher concentrations.

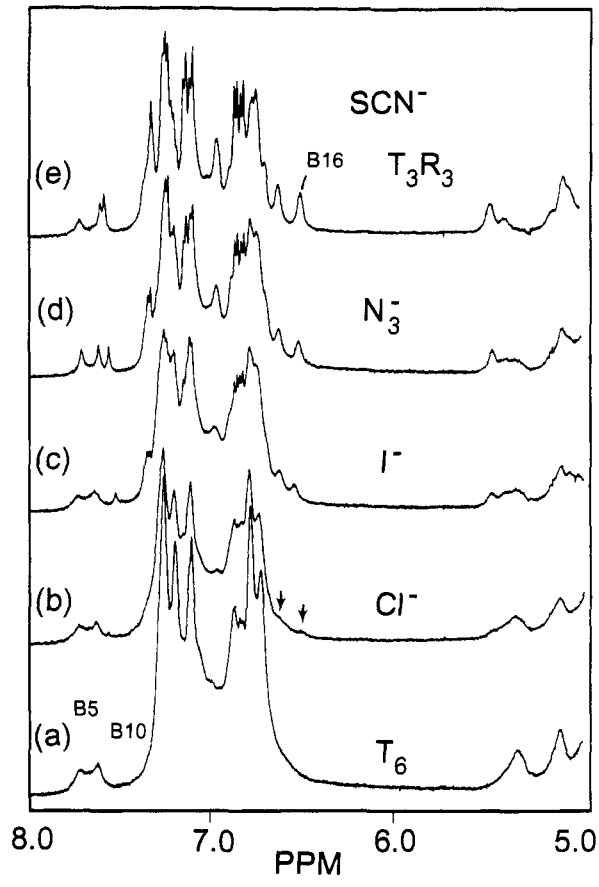

FIGURE 4: ^{1}H NMR spectra at 500 MHz comparing the effects of inorganic anions on the T to R transition of the wild-type zinc–calcium–insulin hexamer in ^2H_2O at pH* 8.0 and 25 °C. Spectra were measured in the presence of the following added anions: (a) none; (b) 50 mM Cl^- (as NaCl); (c) 50 mM I^- (as NaI); (d) 50 mM N_3^- (as NaN_3); (e) 50 mM SCN^- (as NaSCN). All samples were comprised of a [Zn^{2+}]:[Ca^{2+}]:[insulin monomer] = 2:1:6; [insulin monomer] = 3 mM. The appearance of resonances (as peaks or shoulders) at 5.4–5.6 ppm and at 6.4–6.7 ppm and alterations of the HisB5 and HisB10 C2 proton resonances at 7.5–7.8 ppm are characteristic of the presence of R-state hexamer species.

Effects of Anions on T to R Conformational Transition. The spectra presented in Figure 4 compare the effects of Cl^- (b), I^- (c), SCN^- (d), and N_3^- (e) on the ^{1}H NMR spectrum of the zinc–insulin hexamer. The spectrum of Zn(II)–T_6 (a) in the absence of monovalent anions is also presented. In previous work, it has been suggested that the spectrum obtained in the presence of high SCN^- concentrations (>40 mM) is due to a Zn(II)–T_3R_3 species where SCN^- is coordinated to the HisB10 site of the R_3 unit (in a tetrahedral geometry) (Bradbury & Ramesh, 1985; Palmieri et al., 1988). The SCN^- spectrum (d) contains signatures that are similar to those which characterize the Zn(II)–R_6 complex. Further addition of KSCN above 40 mM does not significantly alter the spectrum. Titration of phenol into the SCN^- complex identifies the resonance at 6.55 ppm as belonging to TyrB16. Furthermore, the area under the TyrB16 peak doubles upon saturation with phenol. These findings are consistent with the interpretation that SCN^- stabilizes the T_3R_3 state of the insulin hexamer in solution, while the binding of phenol drives the hexamer toward an R_6 hexamer of higher symmetry. The N_3^- (e) and I^- (c) spectra exhibit similar resonances between 5.0 and 6.7 ppm, and close inspection of the Cl^- system (b) indicates that although this solution is dominated by the Zn-(II)–T_6 species, a small amount of a similar R-state species is present as indicated by the presence of a small shoulder in

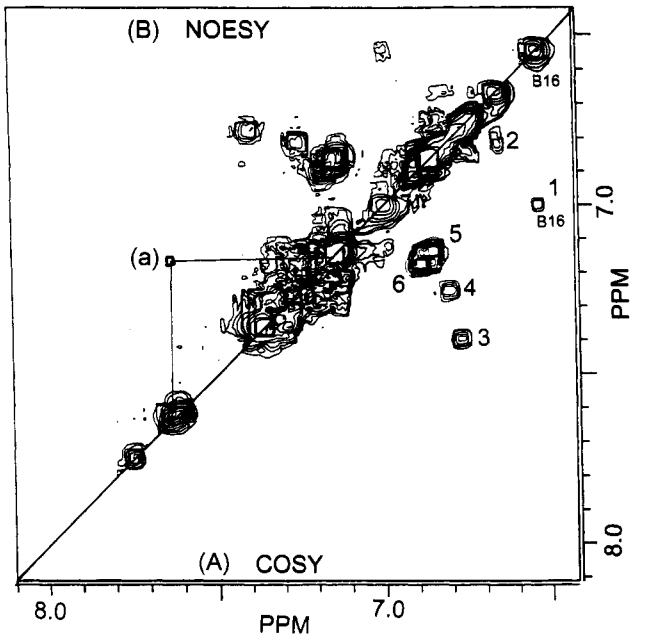

FIGURE 5: Absolute value COSY (A) and NOESY (B) spectra in ^2H_2O at 500 MHz for the Zn(II)–R_6 SCN^- complex of the wild-type human insulin hexamer at pH* 8.0 and 25 °C. Conditions: $[Zn^{2+}]$:$[Ca^{2+}]$:[insulin monomer] = 2:1:6 and $[SCN^-]$ = 50 mM. The NOESY cross peak between the resonances at 7.17 and 7.64 ppm (a) is characteristic of the SCN^--induced T_3R_3 species as are the six Tyr COSY cross peaks (designated 1–6).

the Zn(II)–T_6 spectrum located between 6.6 and 6.8 ppm that could be due to a trace of the R-state conformation. The spectra in Figure 4 indicate that all four anions shift the solution equilibrium away from the T_6 state toward a hexamer that contains monomers with an R-state conformation. By analogy with SCN^-, anions likely stabilize the T_3R_3 conformation of the insulin hexamer. The relative order of effectiveness is $SCN^- > N_3^- > I^- \gg Cl^-$.

Figure 5 compares the aromatic regions of the COSY (A) and NOESY (B) spectra of the SCN^- complex. The COSY spectrum is consistent with the classification of six cross peaks (designated peaks 1–6) located at 6.55, 6.68, 6.77, 6.82, 6.86, and 6.90 ppm as due to *J*-coupling between the 2,6 and 3,5 protons for each of the four Tyr residues found in insulin. The presence of six cross peaks is consistent with a mixture of insulin hexamers that contain both T- and R-states where two of the four Tyr residues reside in different environments (T and R). The chemical shifts of Tyr residues in the T-states are remarkably similar to those reported for certain monomeric insulin mutants (Roy et al., 1990). All but one of the NOESY cross peaks also occurs in the COSY spectrum. The unique NOESY cross peak correlates a HisB10 C2 proton with another aromatic proton, most likely the C4 proton of HisB10.

Roy et al. (1989) reported that both the metal-free and the Zn(II)-substituted GlnB13–insulin hexamers can undergo the phenol-induced T_6 to R_6 conformational transition. Figure 6a compares the 1-D ^1H NMR spectra of the Zn(II)–T_6 GlnB13 mutant (a) with the spectra of the corresponding phenol-induced Zn(II)–R_6 species (b) and the SCN^--induced species (c). The spectrum of the phenol-induced Zn(II)–R_6 species is highly similar to the spectra of the phenol-, resorcinol- or *m*-cresol-induced Zn(II)–R_6 species derived from native human insulin (viz., Figures 2 and 3). The SCN^--induced species obtained with the GlnB13 mutant exhibits a spectrum with characteristic R-state signatures. Inspection of Figure 6 (spectrum c) reveals several notable differences with the wild-type SCN^- spectrum (compare with Figures 4 and 5).

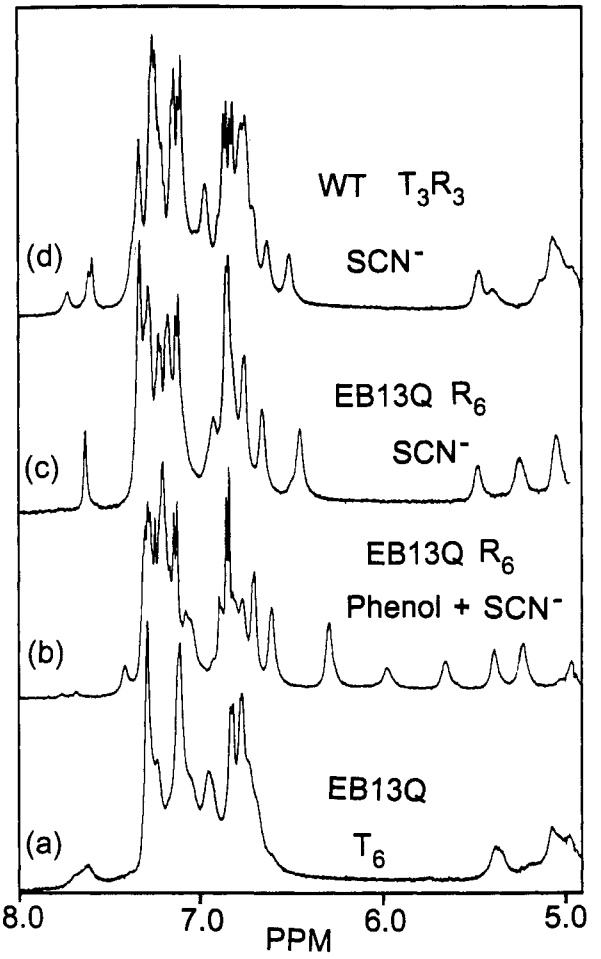

FIGURE 6: Comparison of the effects of phenol and SCN^- on the ^1H NMR spectra of the EB13Q mutant and wild-type human zinc–insulin hexamers in ^2H_2O at pH* 8.0 and 25 °C. (a) EB13Q mutant Zn(II)–T_6; (b) phenol-induced EB13Q mutant Zn(II)–R_6 SCN complex, [phenol-d_6] = 20 mM and $[SCN^-]$ = 50 mM; (c) SCN^--induced EB13Q Zn(II)–R_6 SCN^- complex, $[SCN^-]$ = 50 mM; (d) SCN^--induced wild-type Zn(II)–T_3R_3 SCN^- complex, $[SCN^-]$ = 50 mM).

The His C2 proton region of the B13 mutant spectrum gives a single sharp resonance at 7.68 ppm, whereas native human insulin (Figure 6, spectrum d) gives three His resonances located at 7.61, 7.63, and 7.75 ppm. The mutant complex gives what appear to be single resonances for the peaks located at 5.08, 5.27, and 5.51 ppm, while the corresponding peaks in the spectrum of native human insulin exhibit poorly resolved shoulders. In contrast to the native system data, the COSY spectrum of this mutant (data not shown) is characterized by only four cross peaks located at 6.47, 6.68, 6.78, and 6.87 ppm derived from the *J*-coupling of the Tyr 2,6 and 3,5 protons. Addition of phenol to the EB13Q–SCN^- complex shifts the position of the TyrB16 peak upfield to 6.33 ppm (Figure 6, spectrum b), as is observed for the wild-type complex, but does not alter the area under the TyrB16 resonance. Consistent with this interpretation, the COSY spectrum of the EB13Q–SCN^- complex exhibits only four COSY cross peaks identifiable as Tyr aromatic protons (data not shown), whereas the native protein SCN^- complex exhibits six (Figure 5). Consequently, it appears that SCN^- drives the GlnB13 mutant hexamer completely to an Zn(II)–R_6 species, whereas the native protein forms a hexamer consisting of approximately equal amounts of T- and R-state species.

Evidence for a Phenol-Induced Zn(II)–T_3R_3 Chloride Complex. The series of 1-D ^1H NMR spectra presented in

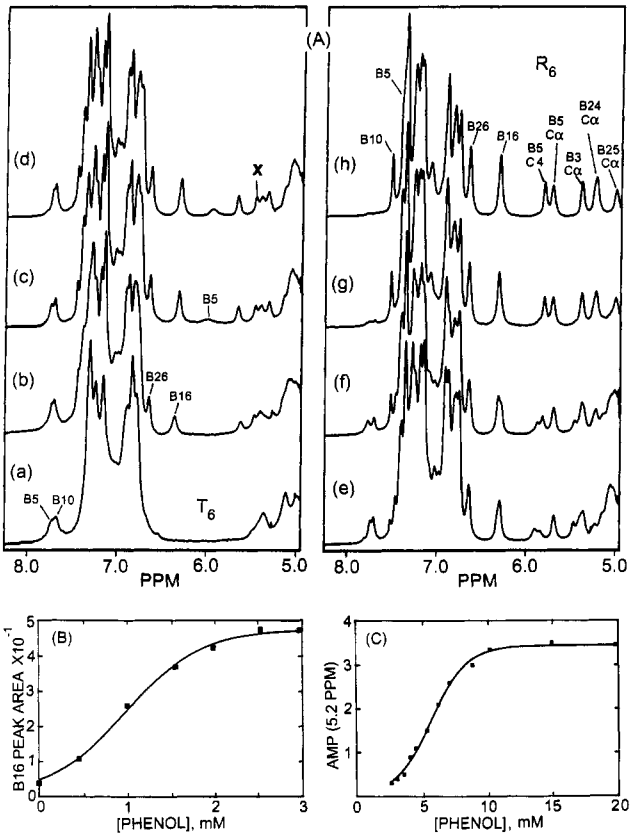

FIGURE 7: (A) Dependence of the 500 MHz ^{1}H NMR spectrum of the wild-type zinc–insulin hexamer on the concentration of phenol-d_6 in ^2H_2O at pH* 8.0 and 25 °C. Conditions: 3 mM insulin (monomer); $[Zn^{2+}]$:$[Ca^{2+}]$:[insulin monomer] = 2:1:6; 50 mM NaCl. Phenol-d_6 concentrations: (a) 0; (b) 0.5, (c) 1.5, (d) 3.0, (e) 4.0 (f) 7.0, (g) 10.6, and (h) 20 mM. Spectra a and h are assigned as the Zn(II)–T_6 species and the Zn(II)–R_6 chloride adduct, respectively. Close inspection of the spectra indicate that the T to R transition is a three-state process (compare spectra a, e, and h). (B) Titration showing the dependence of the area of the TyrB16 3,5 proton resonance on the concentration of phenol-d_6. The midpoint occurs at ~1.1 mM total phenol. (C) Titration showing the dependence of the amplitude of the 5.2 ppm resonance on the concentration of phenol-d_6. The midpoint is located at ~6 mM.

Figure 7A record the spectral changes that occur when the zinc–insulin hexamer is titrated with phenol at pH* 8.0. As the phenol concentration is increased from 0 (spectrum a) to 20 mM (spectrum h), the hexamer is transformed from Zn(II)–T_6 to Zn(II)–R_6 (Roy et al., 1989). In the presence of Ca^{2+} (1 mol/hexamer) and Cl^- ion, the spectra of both the T_6 and the R_6 species (as judged by line widths and the absence of shoulders) are improved. As previously documented here and in earlier publications, the Zn(II)–T_6 species and the phenol-induced Zn(II)–R_6 species are characterized by very different ^{1}H NMR spectra (compare spectrum a with spectrum h). If phenol induces a conformational transition between these two species only (that is slow with respect to the NMR time scale), then at intermediate phenol concentrations the spectra obtained should be weighted composites of the spectra of the interconverting Zn(II)–T_6 and Zn(II)–R_6 species. Careful inspection of the spectra presented in Figure 7A show this is not the case. For example, the appearance of the resonance due to the 3,5 protons of TyrB16 at ~6.25 ppm precedes the appearance of the resonance due to the HisB5 ring C4 proton at ~5.90 ppm. Furthermore, as phenol is titrated into the sample, the resonance from the TyrB16 3,5 protons first moves upfield, shifting from 6.39 (spectrum b) to 6.30 ppm (spectrum d), and then shifting back downfield to 6.35 ppm. The HisB5 C4 proton initially is observed as a very broad peak centered at 6.04 ppm (spectrum c) that shifts upfield to 6.00 ppm (spectrum d), then splits into two peaks (spectra e–g), and finally becomes a single peak centered at 5.82 ppm (spectrum h). The Zn(II)–R_6 spectrum shows a resonance located at 5.25 ppm, which likely corresponds to a Phe Cα proton. This resonance only begins to appear in spectrum e after 4.0 mM phenol has been added. The changes in the His C2 proton region of the spectrum are similarly consistent with the presence of at least three major species during the titration. This progression of spectral changes requires that the conversion of Zn(II)–T_6 to Zn(II)–R_6 involves three species of the hexamer: the initial Zn(II)–T_6 species (spectrum a), the final Zn(II)–R_6 species (spectrum h), and a third species that dominates spectrum d.

Figure 7B presents the initial portion of the dependence of the area under the ~6.25 ppm resonance (the TyrB16 3,5 protons) on the concentration of phenol. The complete titration is biphasic with the initial portion (0–3.0 mM phenol) sigmoidal in appearance. Figure 7C shows the dependence of the amplitude of the 5.25 ppm resonance on the concentration of phenol. This curve also is sigmoidal; however, this transition lags behind the sigmoidal transition charted by the changes in the area under the TyrB16 resonance (Figure 7B). This plot provides further evidence consistent with a mechanism that involves two conformational transitions.

DISCUSSION

The dramatic structural changes (of nearly 30 Å) that occur in the T to R transition of the insulin hexamer, the determination of high-resolution crystal structures (1.5–1.8 Å) of T_6, T_3R_3, and R_6 species, and the symmetry of these protein complexes make the insulin hexamer a unique and valuable system with which to investigate allosteric conformational changes in proteins (Chothia et al., 1983; Baker et al., 1988; Derewenda et al., 1989; Kaarsholm et al., 1989; Roy et al., 1989; Brader et al., 1991; Smith & Dodson, 1992a,b; Choi et al., 1993; Ciszak & Smith, 1994). Two conformational states, designated T_6 and R_6, are pseudo symmetric hexamers. Each has an exact 3-fold symmetry axis along which two Zn^{2+} ions and one central Ca^{2+} ion are located (Sudmeier et al., 1981; Hill et al., 1991). These metal ions significantly stabilize the hexameric form of insulin. Secondly, there are three pseudo 2-fold symmetry axes in the protein complex (Baker et al., 1988; Derewenda et al., 1989; Smith & Dodson, 1992a,b). In the R-state, the symmetry of backbone secondary structural elements are generally conserved, but there are regions where the conformations of residue side chains exhibit pronounced deviations from canonical 2-fold symmetry (Derewenda et al., 1989; Smith & Dodson, 1992a,b). In the T-state, the 2-fold symmetry of secondary structural elements is only roughly conserved (Baker et al., 1988). Finally, in the T_3R_3 conformational state, the pseudo 2-fold symmetry axes are completely lost and only the 3-fold axis remains (Smith et al., 1984; Derewenda et al., 1991; Ciszak & Smith, 1994). Consequently, it is useful to conceptualize the T_3R_3 hexameric species as two halves or two trimeric units. Thus, in the T_3R_3-state, half has undergone the large conformational change characteristic of the R-state, while the other half remains in a conformation characteristic of the T-state.

In previous studies, it has been unclear as to whether the observed asymmetry found in crystalline insulin hexamers is present in solution or if this asymmetry arises as an artifact of the crystallization conditions and crystal packing forces (Smith et al., 1984; Renscheidt et al., 1984; Wollmer et al.,

1987, 1989; Kaarsholm et al., 1989; Choi et al., 1993). The data presented herein establish that the three conformational states observed in crystals (T_6, T_3R_3, and R_6) are indicative of the sequential conformational transitions involved in the T to R conformational change in solution. (As described below, previous studies were performed under solution conditions that *a priori* generate heterogeneous populations of insulin hexamers.) Secondly, asymmetry in the insulin hexamer serves to greatly influence the allosteric properties of the T to R conformation transition. We propose that the observed allosteric conformational changes may be interpreted within the context of a concerted model which incorporates both positive and negative cooperative interactions. The data presented show that each half of the insulin hexamer undergoes a positive cooperative transition from a T-state to an R-state type structure (Figure 7). However, structural asymmetry between halves of the hexamer, whether preexisting or induced, creates two classes of ligand binding sites and results in negative cooperative interactions between the two halves of the hexamer. In the extreme, such structural asymmetry results in the formation of a stable intermediate with a thermodynamic barrier that prevents certain ligands from inducing the complete conversion from the T-state to the R-state. Instead, these ligands (viz., SCN^-, Figures 4–6) stabilize only the T_3R_3 conformational state. However, mutation of GluB13 to Gln, a residue that exhibits large deviations from 2-fold symmetry in the hexamer, effectively lowers this barrier and not only facilitates the phenol-induced T_6 to R_6 transition but also allows for complete conversion by SCN^- to the R_6 state (Figure 6).

Anions Are Positive Heterotropic Effectors for Phenol-Mediated T to R Conformational Transition. Ligand binding to the phenolic pocket, the T to R conformational transition, and heterotropic anion effects are very tightly linked functions. The crystallographic evidence identifies only a single binding locus for anion effectors, the fourth coordination position of the R-state HisB10 metal sites. The only other evidence for additional anion binding sites is the finding that the HisB10 site of the T_3 unit of certain T_3R_3 species has a weak affinity for Cl^- (Smith & Ciszak, 1994). Thus, at the high Cl^- concentrations used in the crystallization of T_3R_3, the metal site of the T_3 unit is disordered; analysis of the electron density maps indicates the presence of comparable amounts of an octahedral geometry (three HisB10 and three H_2O ligands) and a tetrahedral geometry (three HisB10 and one Cl^-). It seems unlikely that the HisB10 site of a T_3 unit plays any significance in the anion binding effects described herein.

Assignment of Aromatic Region of R-State Insulin Hexamer. Table 1 lists the sequence-specific assignments of the aromatic region of the resorcinol-induced R_6 state of the 2Zn–insulin hexamer (see Results for a complete description of assignments). The assignments are consistent with predictions based on the R_6 state crystal structure of the phenol complex (Derewenda et al., 1989; Smith & Dodson, 1992a,b). TyrB16 and the HisB5 and HisB10 resonances could be assigned independent of crystallographic information (Figure 3, Table 1). The pattern of observed NOEs between these residues and the remaining aromatic protons (Figure 3), in conjunction with the crystal structure, were sufficient to assign the remainder of the aromatic region. Minor uncertainties remain that are due to the chemical shift degeneracy of specific protons in the aromatic region.

The 1-D and 2-D NMR spectra of the R_6 state induced by ligands other than resorcinol are very similar to the corresponding spectra of the resorcinol complex. The primary difference lies in the chemical shifts of HisB5 resonances. Variation of the position of B5 resonances with ligand structure almost certainly results from changes in anisotropic ring current effects with different aromatic ligands. These differences likely are a result of either minor changes in the position of the bound ligand or small changes in the conformation of the ligand binding pocket necessary to accommodate the steric requirements of different aromatic ligands. If the nonaromatic ligand, cyclohexanol, is used to induce the R-state of the insulin hexamer, then the B5 resonance located between 6 and 5.7 ppm found in the spectra of R_6 species induced by aromatic ligands is not observed in this region of the spectrum (data not shown).

The other resonances observed between 5 and 6 ppm (Figures 2 and 3) are particularly interesting. Integrations of the intensities of these peaks give relative areas equivalent to approximately one proton each, a finding consistent with the assignment of these resonances to Cα protons (Table 1). The resonances located at 5.23 and 5.0 ppm exhibit strong cross peaks to the aromatic protons of PheB24 and PheB25 (Figure 3). The peak positions are consistent with Cα protons residing in a β-sheet region of the protein. In the insulin hexamer, residues B24–B26 form part of the antiparallel β-pleated sheet structure at the monomer–monomer interface. On the basis of these considerations, we propose that the resonances located at 5.0 and 5.23 ppm correspond to the Cα protons of PheB25 and PheB24, respectively. Another interesting observation is that the relative ratios of these peaks suggest an asymmetry of the PheB25 residue, consistent with that observed in the crystal structures of both R-state and T-state insulin hexamers. This finding indicates that the R_6-state exhibits some deviations from perfect 2-fold symmetry in solution.

The resonances at 5.7 and 5.4 ppm are upfield shifted but show no strong NOEs to aromatic residues. Instead, there are NOEs between these resonances and resorcinol (Figure 3). With the present data, it is difficult to ascertain whether or not these cross peaks represent spin diffusion peaks or real NOE cross peaks. However, the presence of these peaks is not dependent on the nature of the aromatic ligand. These peaks are shifted downfield, even when cyclohexanol is used to stabilize the insulin hexamer R-state (data not shown). Therefore, ring current field effects (attributed either to the ligand, to Tyr, or to Phe residues) cannot account for the observed chemical shifts of these peaks. Another explanation involves the possibility of an interaction between the Cα of HisB5 and the Nδ1 of His B5. The crystal structure indicates that the conformation of this residue places these protons within NOE contact (3–4 Å) aligned along the edge of the His ring. In D_2O, no cross peak with a His ring proton would be observed. Secondly, there is a very weak NOE between the resonance at 5.4 ppm and PheB1. Although this peak probably arises from spin diffusion, this NOE suggests a location that is close to PheB1. Therefore, the most likely possibility is that this resonance arises from a Cα proton within the extended helix composed of residues B1–B8, the region of the protein that undergoes the largest conformational change. Likely candidates include AsnB3 or GlnB4. This assignment is provisional and will require further experimental evidence in order to be verified.

Titration Studies. The T-state is characterized by rather broad, poorly defined resonances (Figures 2 and 4). For instance, the His C2 proton resonances of both HisB5 and HisB10, centered at 7.50 and 7.58, respectively, are very broad, especially when compared to the R-state spectrum. Therefore, in addition to the molecular weight of the complex, the T-state

must exist in multiple conformational or structural equilibria. Such a situation could arise from conformational heterogeneity (as is observed in the T-state crystal structure), from a hexamer in equilibrium with lower molecular weight species, or from an equilibrium with the T_3R_3 conformation of the hexamer. In support of the latter hypothesis, in the presence of 50 mM Cl^-, there is evidence for a minor T_3R_3 component, indicated by the small amplitude of the upfield TyrB16 resonance that appears as an upfield shoulder on the envelope of aromatic resonances at 6.50 ppm (Figure 4). This shoulder is not apparent in the absence of Cl^-.

The sequence-specific assignments of the aromatic region facilitate the interpretation of spectral changes which accompany the phenol-induced T to R transition. Figure 7 shows the large spectral changes which occur during the T to R conformational transition. These results clearly demonstrate that the conformational change involves at least three separate conformational states. This behavior is particularly clear from inspection of the TyrB16, HisB5, and HisB10 resonances. The upfield shift of TyrB16 plateaus at approximately 2 mM phenol. At higher phenol concentrations, a new B16 peak is observed immediately downfield. Such closely spaced peaks are indicative of a process in very slow exchange. These data clearly demonstrate that the T to R conformational transition is a negative cooperative process (Figure 7A–C). There are two classes of binding sites for the phenolic ligand. Furthermore, the equilibrium interconversion between the two halves of the insulin hexamer (i.e., $T_3R_3 \rightleftharpoons R_3T_3$) and the interconversion of the T_3R_3 and R_6 conformations also are in the slow exchange regime. Definition of slow exchange on the NMR time scale is determined not only by the rate of interconversion and the magnetic field strength but also by the chemical shift difference ($\tau_m\Delta\omega \gg 1$); where τ_m is the lifetime of a nucleus in a particular environment and $\Delta\omega$ is the chemical shift difference. The TyrB16 3,5 protons and the HisB5 C2 proton resonances each exhibit distinct peaks separated by less than 0.06 ppm (30 Hz). This implies that the lifetime of the complex in a particular conformation must be $\gg$30 ms to be in slow exchange. This conclusion is supported by direct measurement of the rate at which the conversion from octahedral to tetrahedral coordination occurs in the phenol-induced interconversion of T_6 and R_6 for the Co(II)-substituted species (Gross & Dunn, 1992). Therefore, we conclude that exchange between the T_3R_3 and R_6 conformations is very slow.

Close examination of the phenol-induced T to R spectral changes (Figure 7) reveals a number of other resonances which indicate a three-state process. The upfield-shifted HisB5 resonance clearly undergoes a two-phase transition. During the intial stages of the first phase, the C4 ring proton resonance is very broad and ill defined but then sharpens as the first phase is nearly saturated. The line shape and position of this peak is dependent not only on the conformational change but also on the ligand on and off rates. HisB5 forms part of the ligand binding pocket. Several resonances are observed which appear to be specific to the intermediate state at 5.4 and 7.4 ppm. These could also be T-state resonances in the T_3R_3 hexamer that are no longer exchange-broadened. During the second phase of the titration in which the intermediate state is converted to the R_6 conformation, a second, distinct resonance is observed that is in slow exchange. Several resonances are observed that are distinct to the R_6-state. These include the resonance at 5.23 ppm and the HisB10 resonance at 7.50 ppm.

The area of the TyrB16 resonance plotted versus phenol concentration is shown in Figure 7B. The transition is sigmoidal, indicative of a cooperative conformational transition. Molecular modeling studies (O. Olsen, personal communication) show that the subunits of the trimeric units of the insulin hexamer cannot undergo the coil to helix transition sequentially; therefore, a high degree of cooperativity is expected in the T to R transition. Choi et al. (1993) report Hill coefficients as large as 2.8 for the ligand-induced conformational change. A plot of the dependence of signal intensity for the resonancee at 5.23 ppm on the phenol concentration is shown in Figure 7C. Since the transition from the intermediate state to the R_6 state is in very slow exchange, the line width of this resonance does not significantly change during this phase of the titration. Again, the second phase of the titration exhibits a sigmoidal concentration dependence, indicative of a positive cooperative transition. Therefore, the transition of each trimer must be a positive cooperative process, but the interactions between the two halves of the hexamer produce two classes of phenol binding sites, a behavior indicative of negative cooperative interactions between the two halves of the insulin hexamer.

Evidence That the Intermediate State Is a T_3R_3 Complex. At 2 mM phenol, the area under the TyrB16 resonance at ~6.30 ppm is almost exactly one-half of the corresponding area measured in the R_6 state (Figure 7A,B). This observation limits the possible mechanisms. For example, transitions which involve stable intermediates where only one or two subunits have undergone the T to R transition are eliminated. As expected, the interaction of HisB5 and TyrB26 with TyrB16 in the T_3R_3 and R_6 states dramatically alters the chemical shift of the B16 resonance. The position of this resonance in the T-state is similar to that found in certain monomeric insulins at a similar pH (Roy et al., 1990; Kadima et al., 1992). Further experiments are currently underway to identify the position of other resonances, particularly Cα protons, in the T_3R_3 state of the insulin hexamer.

Role of Asymmetry in the T to R Conformational Transition. Comparisons of the crystal structures of the various conformational states of the insulin hexamer show a number of sites where symmetry is not conserved. One residue of particular interest to these studies is GluB13. This is the single residue of the protein where the side chains from all monomers are in close proximity to one another. Secondly, the asymmetry of this residue is clearly seen in the various conformational states (Figure 7). The GluB13 carboxyl group has been shown to form interesting H-bonding interactions with other B13 carboxyl groups (the pK_a of B13 is significantly increased in the hexameric state; Kaarsholm et al., 1990), the GluB13 carboxylates form a novel Ca^{2+} binding site (Sudmeier et al., 1981; Storm & Dunn, 1985; Hill et al., 1991), and this residue has the potential to form strong H bonds with the hydroxyl group of SerB9, particularly in the R-state form of the hexamer (both in the T_3R_3 and R_6 conformations). Mutation of GluB13 to Gln greatly alters electrostatic interactions and may be expected to change the H-bonding patterns of this residue. Although the crystal structures of the native hexamer and the GlnB13 mutant do not reveal large changes in the position of this side chain (Derewenda et al., 1989; Smith & Dodson, 1992a,b; Bentley et al., 1992), the NMR data establish that this mutation greatly lowers a thermodynamic barrier, allowing ligands, such as KSCN, to induce complete conversion to the R-state. Whereas in the native protein the SCN^--induced conformational transition progresses only to the T_3R_3 state, the GluB13 mutant is capable of a complete T_6R_6 transition in the presence of SCN^- alone.

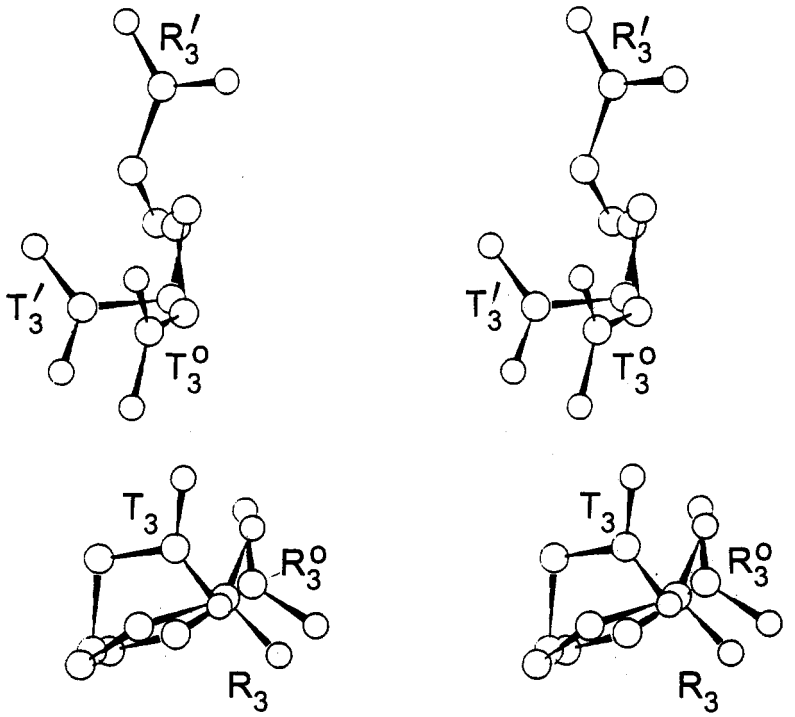

FIGURE 8: Stereo drawings comparing the conformations assumed by the GluB13 side chains in the T_3T_3', $T°_3R°_3$, and R_3R_3' structures of the insulin hexamer. The insulin dimers shown in Figure 1A–C were superimposed, and the orientation of the GluB13 side chains with each dimer are shown. The perspective is identical to that shown in Figure 1A–C with the pseudo 2-fold symmetry axis oriented perpendicular to the plane of the page. Individual residues from different monomeric units are labeled according to Scheme 1.

Modeling Allosteric Properties of the Insulin Hexamer. Previous spectroscopic and kinetic studies of the insulin hexamer in solution (Kaarsholm et al., 1989; Gross & Dunn, 1992; Brader et al., 1991; Choi et al., 1993; Bloom et al., 1994) and the crystal structures of T_6, T_3R_3, and R_6 species (Derewenda et al., 1989; Smith & Dodson, 1992a,b; Bentley et al., 1992; Ciszak & Smith, 1994) provide strong evidence against an induced fit mechanism (Koshland et al., 1966) involving species of low symmetry (i.e., the species T_5R_1, T_4R_2, T_2R_4, and T_1R_5). The negative cooperative behavior of the system rules out the concerted model of Monod et al. (1965). Consequently, a model capable of both negative and positive cooperative behavior would appear a suitable choice for describing the properties of the insulin hexamer.

A crystalline T_3R_3 species was first reported in 1976 (Bentley et al., 1976). Further details of this structure were provided in 1984 and in 1994 (Smith et al., 1984; Ciszak & Smith, 1994). More recently, it has been shown that the phenol analogues, *N*-acetyl-*p*-aminophenol (G. D. Smith, private communication), *p*-hydroxybenzamide (G. D. Smith and M. E. Dunn, unpublished results), *p*-hydroxyethylbenzoate, and the SCN^- adduct of human insulin (G. G. Dodson, private communication), all give crystalline T_3R_3 species. The single-chain insulin species human B29–A1 insulin (Derewenda et al., 1991) also gives a crystalline T_3R_3 species. Whereas the only crystalline R_6 species thus far reported are the phenol complexes (Derewenda et al., 1989; Smith & Dodson, 1992a,b), the *m*-cresol complex, and the resorcinol complex (G. D. Smith, private communication).

The structural asymmetry of the R_6 state gives rise to two slightly different classes of phenolic pockets (Derewenda et al., 1989; Smith & Dodson, 1992a,b). Comparison of R_6 structures with T_3R_3 structures (viz., Figure 8) shows that the phenolic pockets of the R_3 unit of T_3R_3 are significantly different in structure from either conformation found in the R_6 structures. Some of these structural differences may be localized ligand-induced effects that reflect the plasticity of the pocket. However, the crystallographic evidence is consistent with at least three classes of R-state conformations. Figure 8 illustrates the differences in conformation for these three states by comparing the conformations of the GluB13 side chain for molecules 1 and 2 of T_6 with T_3R_3 and R_6. The evidence that mutation of GluB13 to Gln (viz., Figures 4–6 and Roy et al., 1989; Bloom et al., 1994) substantially alters the thermodynamics of the interconversions of T_6, T_3R_3, and R_6 in favor of R_6 formation implies that the interactions in wild-type insulin that convey stability to the highly asymmetric structure of T_3R_3 include contributions from the GluB13 carboxylates. The EB13Q mutation (at least in part) alleviates the structural constraints that cause the wild-type R_6–SCN^- complex to be a significantly higher energy species.

This work and the studies of Bloom et al. (1994) demonstrate that the interconversion of T_6 and R_6 occurs via a T_3R_3 intermediate and that the process is composed of both positive and negative cooperative allosteric transitions. This behavior is consistent with the structural asymmetry SMB model (Seydoux et al., 1974; Matthews & Bernhard, 1973). This model provides a rationale, both for the negative and positive cooperative behavior and the apparent half-of-the-sites reactivity that is grounded in the structural asymmetry of the hexamer. Therefore, we postulate that the mechanism of the allosteric transition occurs via the SMB model, as depicted in Scheme 1. This model predicts that the structural asymmetry of the R_6 state must give rise to two classes of phenolic pockets distinguished by different structures and different affinities for ligands, a prediction consistent with the observed differences in the structures of the phenolic pockets of T_3R_3 and R_6 species (Derewenda et al., 1989; Smith & Dodson, 1992a,b; G. D. Smith, private communication). Therefore, here and in the discussion which follows, it is necessary to explicitly recognize the suboptimal symmetry of

Scheme 1: Mechanism Proposed To Describe Homotropic Effects of Phenolic Ligands (P) on T to R Allosteric Transitions of Insulin Hexamer[a]

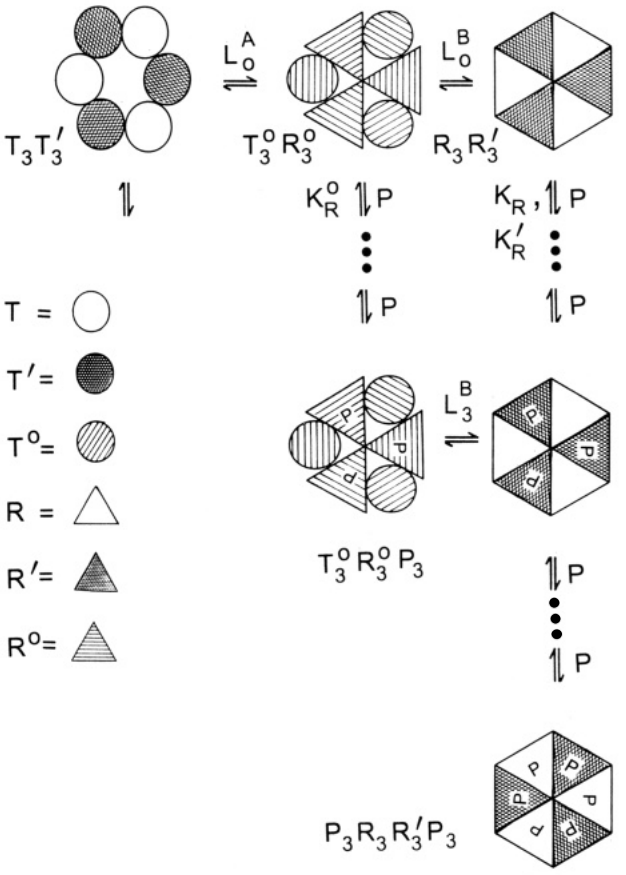

[a] The model is defined by two allosteric constants (L_O^A and L_O^B), three dissociation constants for binding to R-state species (K_R, K'_R, and $K°_R$), and [using a modification of the nomenclature proposed by Kaarsholm et al. (1989)] six different subunit conformations (designated T, T′, T°, R, R′, and R°). In this scheme, the affinities of subunits with T-state conformations for phenolic ligands are assumed to be negligible. For brevity, only some of the possible (R-state) liganded species and binding equilibria are depicted.

T_6 and R_6 and the conformational differences among the R_3 units of T_3R_3 and R_6; accordingly, these species are referred to as T_3T_3', $T°_3R°_3$, and R_3R_3', respectively (Scheme 1).

The magnitudes of the allosteric constants

$$L_A = \frac{[T_3T'_3]}{[T_3R°_3]}$$

and

$$L_B = \frac{[T°_3R°_3]}{[R_3R'_3]}$$

and the dissociation constants for ligand binding to the six subunit conformations, $K°_T$, K_T, K_T', $K°_R$, K_R, and K_R', determine the cooperativity (positive, negative, mixed, or noncooperative) of the system. Thus, if $L_A > 1$ and $L_B > L_A$; if $K°_T$, K_T, $K_T' \gg K°_R$, K_R, and K_R'; and if $K_R \simeq K_R'$, then the ligand binding isotherms will consist of two sigmoidal phases of equal amplitudes. The titration shown in Figure 7, where the concentration of phenol is varied, indicates such behavior. As a consequence of the preferential stabilization of the R_3R_3' state, positive heterotropic effectors will shift these sigmoidal phases toward hyperbolic limits wherein the negative cooperativity of the system is obscured. Thus, Choi et al. (1993) reported that anions such as Cl^- and SCN^- shift the sigmoidal binding curves obtained with phenol and the phenol analogues, resorcinol, *m*-cresol, and *p*-hydroxybenzamide, toward a hyperbolic limit and that the strength of the heterotropic effect parallels the relative affinities of the heterotropic anion (Cl^-, SCN^-, or phenolate ion) for the R-state. Detailed application of this model to the ligand-induced allosteric transition for both the wild-type and E13Q hexamers is currently in progress (Bloom et al., 1994).

ACKNOWLEDGMENT

We thank Dr. O. Olsen for informing us of the results of his molecular dynamics simulations of the T to R transition prior to publication, and we thank Drs. A. Bloom and S. Ludvigsen for help in the collection of the 600-MHz NMR spectra.

REFERENCES

Baker, E. N., Blundell, T. L., Cutfield, J. F., Cutfield, S. M., Dodson, E. J., Dodson, G. G., Hodgkin, D. C., Hubbard, R. E., Isaacs, N. W., Reynolds, C. D., Sakabe, K., Sakabe, N., & Vijayan, N. M. (1988) *Philos. Trans. R. Soc. London, B 319*, 369–456.

Bentley, G. A., Dodson, E. J., Dodson, G. G., Hodgkin, D. C., & Mercola, D. A. (1976) *Nature 261*, 166–168.

Bentley, G. A., Brange, J., Derewenda, Z., Dodson, E. J., Dodson, G. G., Markussen, J., Wilkinson, A. J., Wollmer, A., & Xiao, B. (1992) *J. Mol. Biol. 228*, 1163–1176.

Bloom, C. R., Choi, W. E., Brzović, P. S., Ha, J. J., Huang, S.-T., Kaarsholm, N. C., & Dunn, M. F. (1994) (submitted for publication).

Blundell, T., Dodson, G., Hodgkin, D., & Mercola, D. (1972) *Adv. Protein Chem. 26*, 279–402.

Bodenhausen, G., Kogler, H., & Ernst, R. R. (1984) *J. Magn. Reson. 58*, 370–388.

Bradbury, J. H., & Ramesh, V. (1985) *Biochem. J. 229*, 731–737.

Bradbury, J. H., Ramesh, V., & Dodson, G. (1980) *J. Mol. Biol. 150*, 609–613.

Brader, M. L., & Dunn, M. F. (1991) *Trends Biochem. Sci. 16*, 341–345.

Brader, M. L., Kaarsholm, N. C., & Dunn, M. F. (1990) *J. Biol. Chem. 265*, 15666–15670.

Brader, M. L., Kaarsholm, N. C., Lee, W.-K., & Dunn, M. F. (1991) *Biochemistry 30*, 6636–6645.

Brader, M. L., Borchardt, D., & Dunn, M. F. (1992) *Biochemistry 31*, 4691–4696.

Choi, W., Brader, M. L., Aguilar, V., Kaarsholm, N. C., & Dunn, M. F. (1993) *Biochemistry, 32*, 11638–11645.

Chothia, C., Lesk, A. M., Dodson, G. G., & Hodgkin, D. C. (1983) *Nature 302*, 500–505.

Ciszak, E., & Smith, G. D. (1994) *Biochemistry 33*, 1512–1517.

Conway, A., & Koshland, D. E., Jr. (1968) *Biochemistry 7*, 4011–4023.

Corwin, L. M., & Fanning, G. P. (1968) *J. Biol. Chem. 243*, 3517–3525.

Derewenda, U., Derewenda, Z., Dodson, E. J., Dodson, G. G., Reynolds, C. D., Smith, G. D., Sparks, C., & Swensen, D. (1989) *Nature 338*, 594–596.

Derewenda, U., Derewenda, Z., Dodson, E. J., Dodson, G. G., Bing, X., & Markussen, J. (1991) *J. Mol. Biol. 220*, 425–433.

Gross, L., & Dunn, M. F. (1992) *Biochemistry 31*, 1295–1301.

Hill, C. P., Dauter, Z., Dodson, E. J., Dodson, G. G., & Dunn, M. F. (1991) *Biochemistry 30*, 917–924.

Jeener, J., Meier, B. H., Bachmann, P., & Ernst, R. R. (1979) *J. Chem. Phys. 71*, 4546–4553.

Kaarsholm, N. C., Ko, H.-C., & Dunn, M. F. (1989) *Biochemistry 28*, 4427–4435.

Kaarsholm, N. C., Havelund, S., & Hougaard, P. (1990) *Arch. Biochem. Biophys. 283*, 496–502.
Kadima, W., Roy, M., Lee, R. W.-K., Kaarsholm, N. C., & Dunn, M. F. (1992) *J. Biol. Chem. 267*, 8963–8970.
Koshland, D. E., Jr. (1970) in *The Enzymes*, 3rd ed. (Boyer, P. D., Ed.) Vol 1, p 342, Academic Press, New York.
Koshland, D. E., Nemethy, G., & Filmer, D. (1966) *Biochemistry 5*, 365–385.
Kraulis, P. J. (1991) *J. Appl. Crystallogr. 24*, 946–950.
Marion, D., & Wüthrich, K. (1983) *Biochem. Biophys. Res. Commun. 113*, 967–974.
Matthews, B., & Bernhard, S. A. (1973) *Annu. Rev. Biophys. Bioeng. 2*, 257–317.
Monod, J., Wyman, J., & Changeux, J.-P. (1965) *J. Mol. Biol. 12*, 88–118.
Palmieri, R., Lee, R. W.-K., & Dunn, M. F. (1988) *Biochemistry 27*, 3387–3397.
Porter, R. R. (1953) *Biochem. J. 53*, 320–328.
Rance, M., Sorensen, O. W., Bodenhausen, G., Wagner, G., Ernst, R. R., & Wüthrich, K. (1983) *Biochem. Biophys. Res. Commun. 117*, 479–485.
Renscheidt, H., Strassburger, W., Glatter, U., Wollmer, A., Dodson, G. G., & Mercola, D. A. (1984) *Eur. J. Biochem. 142*, 7–14.
Roy, M., Brader, M. L., Lee, R. W.-K., Kaarsholm, N. C., Hansen, J., & Dunn, M. F. (1989) *J. Biol. Chem. 264*, 19081–19085.
Roy, M., Lee, R. W.-K., Kaarsholm, N. C., Thørgersen, H., Brange, J., & Dunn, M. F. (1990) *Biochim. Biophys. Acta 1053*, 63–73.
Seydoux, F., Malhotra, O. P., & Bernhard, S. A. (1974) *CRC Crit. Rev. Biochem. 2*, 227–257.
Smith, G. D., & Dodson, G. G. (1992a) *Biopolymers 32*, 441–445.
Smith, G. D., & Dodson, G. G. (1992b) *Proteins Struct. Funct. Genet. 14*, 401–408.
Smith, G. D., Swenson, D. C., Dodson, E. J., Dodson, G. G., & Reynolds, C. D. (1984) *Proc. Natl. Acad. Sci. U.S.A. 81*, 7093–7097.
Storm, M. C., & Dunn, M. F. (1985) *Biochemistry 24*, 1749–1756.
Sudmeier, J. L., Bell, S. J., Storm, M. C., & Dunn, M. F. (1981) *Science 212*, 560–562.
Wollmer, A., Rannefeld, B., Johansen, B. R., Hejnaes, K. R., Balschmidt, P., & Hansen, F. B. (1987) *Biol. Chem. Hoppe-Seyler 368*, 903–912.
Wollmer, A., Rannefeld, B., Stahl, J., & Melberg, S. G. (1989) *Biol. Chem. Hoppe-Seyler, 370*, 1045–1053.
Wüthrich, K. (1986) *NMR of Proteins and Nucleic Acids*, p 292, Wiley & Sons, Inc., New York.